

## Geometry Simplification of Wrinkled Wall Semi-rigid Aluminum Containers in Heat Transfer Simulation

H. Vatankhah<sup>1</sup>, N. Zamindar<sup>2\*</sup>, and M. Shahedi<sup>1</sup>

### ABSTRACT

Semi-rigid aluminum containers are being used widely in food industries. They have wrinkle shaped walls for strengthening their physical structure. The objective of this study was to assess the effect of wrinkled parts on the heat transfer and temperature distribution of the containers by Computational Fluid Dynamics (CFD) analysis. Therefore, a precise designed geometry of the wrinkled walls container was compared to a straight one. The analysis was carried out based on the physical properties of a carrot-orange soup. The velocity vectors showed a strong circulation towards the core. The Slowest Heating Zone (SHZ) locations were the same for wrinkled and simplified containers. Average temperature of the symmetric plane and the coldest point of SHZ showed less than 1% difference. The lethality imposed to the SHZ in the wrinkled wall container was about 0.4% more than the straight one. The simulation results revealed that wrinkled walls do not play an important role in increasing heat transfer and as a result, such geometries could be simplified while modeling.

**Keywords:** Can geometry, CFD, Heat transfer, Semi-rigid aluminum container, SHZ, Wrinkled wall.

### INTRODUCTION

Sterilization is the complete destruction or elimination of all viable organisms in/on a food to extend its shelf life. Physical nature of product (food size and shape, product composition and viscosity) and mode of heating (hot water or steam) decide the amount of heat needed for treatment (Ramesh, 2007). Having a sound analysis of the heat transfer mechanism in the canning industry helps us to improve food quality, optimize processing condition and prevent energy loss. Heat transfer mechanisms in a canned food include conduction for solid foods, natural convection, especially for low viscosity liquid foods, convection plus conduction for liquid foods with solid particles, and convection followed by conduction for liquid foods containing starch or high viscosity modifiers (Chen and

Ramaswamy, 2007).

CFD is a simulation tool, which uses powerful computers in combination with applied mathematics to model fluid flow situations and aid in optimal design of industrial processes (Anandharamakrishnan, 2011). It is a good way to predict temperature profile of canned foods during processing (Farid and Ghani, 2004; Ghani *et al.*, 1999, 2003). Several studies have been done to model the temperature pattern during heat treatments based on computational analysis (Datta and Teixeira, 1988; Farid and Ghani, 2004; Naveh *et al.*, 1983; Nicolai *et al.*, 1998; Teixeira *et al.*, 1969).

During thermal process, the temperature inside the food depends on time as well as on the position inside the food system. The design of the thermal process is, therefore, always based on the temperature course in that position in the can that receives the least

<sup>1</sup> Department of Food Science and Technology, College of Agriculture, Isfahan University of Technology, Isfahan, 84156-83111, Islamic Republic of Iran.

<sup>2</sup> Department of Food Science and Technology, Khorasgan Branch, Islamic Azad University, Isfahan, 81551-39998, Islamic Republic of Iran.

\*Corresponding author: e-mail: zamindar@ag.iut.ac.ir



intense heat treatment. Temperature profiles are determined using analytical and numerical solutions of partial differential equations governing the process (Kızıltas *et al.*, 2010). The region that receives the least sterilization in the food product is called the Slowest Heating Zone (SHZ) (Ghani *et al.*, 1999).

Geometry modification of foods seems to be one possible way to increase the heat transfer rate due to changing the distance that heat needs to transfer from outer boundary to the SHZ (Bown and Richardson, 2004).

To achieve sufficient sterility while minimizing cooking in modified shapes of food containers, the temperature distribution patterns should be analyzed (Brody, 2002). Geometry modifications are used to increase the rate of heat transfer from the boundary sides to the SHZ (Bown and Richardson, 2004; Varma and Kannan, 2006). Experimental and computational studies on Toroid cans were carried out by Erdogdu and Tutar (2011), and the results demonstrated the significant effect of additional boundary inside the toroid can to increase the heating rate. Varma and Kannan (2006) compared temperature profiles and movement of SHZ, in a conical geometry, of equal volume and height as that of the cylinder in a computational study. In liquid or semi-fluid food products when the heat transfer mechanism is convection, geometry modification and its orientation are to enhance the heat transfer rate (Varma and Kannan, 2006). Semi-rigid aluminum containers are widely used in Iranian canning industries. These containers have many advantages including ease of handling, variation of shapes and printability.

In this study, the effect of modified wrinkled parts of side walls of semi-rigid aluminum container on heat transfer and temperature distribution of the food container was investigated and compared to plain shaped wall designed geometry of the same dimensions. Since installation of temperature probes would influence the temperature-velocity fields, the fluid motion and hence the temperature distribution in the can (Ghani *et al.*, 2002a; Kumar *et al.*, 1990), a

computational analysis was carried out. In addition, the computational study was based on the thermal sterilization of an orange-carrot soup which had been simulated and validated by Ghani *et al.* (2001).

## MATERIAL AND METHODS

### Geometry and Meshing

Three dimensional symmetric geometries were designed by Ansys geometry designer version 12 (Ansys Inc., USA), based on dimensions of semi-rigid aluminum based packages, Alupak type B 232 made in Switzerland. The length of base (square) face of the container was 88mm while the length of top (square) face was 92.8 mm and the height was 27.5 mm. There was an angle of 95° between can bottom and side walls. On each side there were 6 wrinkled parts, 1 mm inwards the walls. By symmetry one half of the volume with a vertical diagonal cut through the cross section was designed. The first geometry was the real shape of the containers (Figure1) while the second geometry was a simplified form of the container without any wrinkles (Figure 2). The can wall thickness was 0.15 mm and the meshes were designed in 'Ununiform' way. The boundary adjacent to the heated walls and the thickness of that has a very important role in the numerical convergence since temperature and velocity variation is higher than the other regions (Ghani, 2006). For meshing, the edge size of the wrinkle was 0.1 mm and the sizes of other edges were 0.8 mm with a Bios factor of 10. This designing made a denser mesh number near the wrinkled parts (Figure 1). This satisfied the need for having a more precise computation of the effect of wrinkles on the heat transfer inside the container. For the simplified geometry, a 'uniform' 1mm<sup>3</sup> cell mesh was devised. Mesh number was 250904 and 652306 for Straight Walls Container (SWC) and Wrinkled Walls Container (WWC), respectively. The containers were supposed to be filled by the

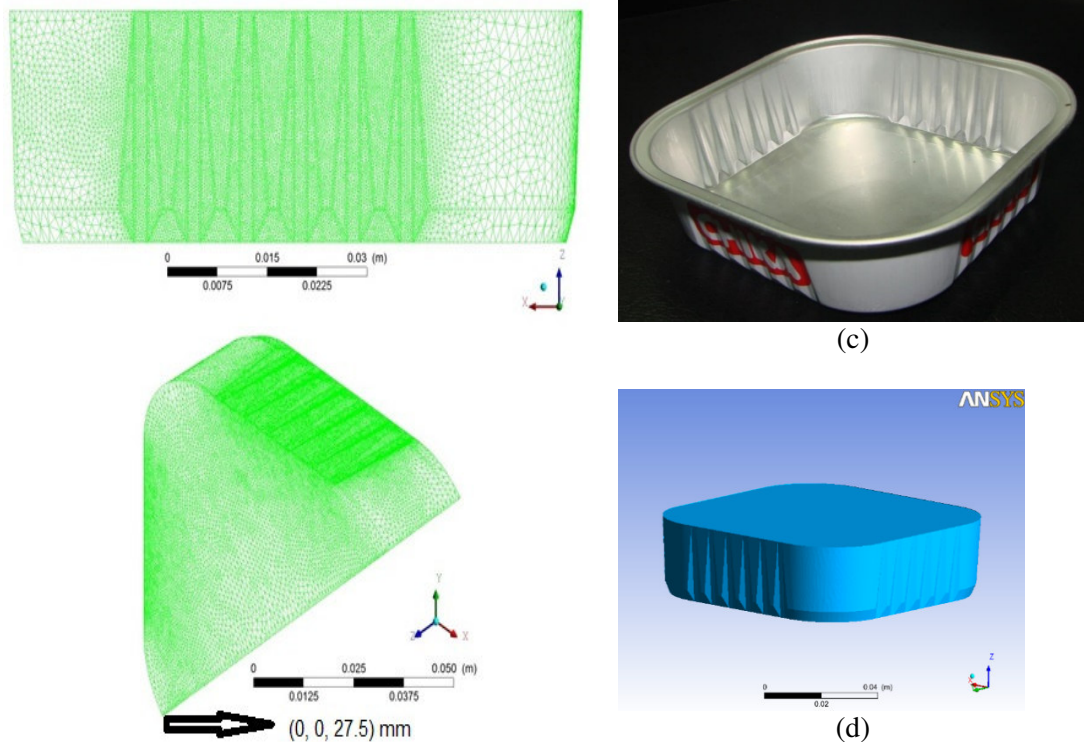


**Figure 1.** Meshed wrinkled wall geometry (a); wrinkled wall container geometry (b); real image of Alupak packaging type B232 (c), designed geometry (d).

product. In other word, using  $1\text{mm}^3$  meshes, like other regions of the geometry, led to complete negligence of the wrinkles' effects. Moreover, triangular meshes were used in WWC; because these kinds of meshes were more flexible and adaptable on awkward shapes such as this study (numerous wrinkles,

complicated geometry, and a  $27^\circ$  slip in the vertical walls). In addition, as described before, a systematic gradual enhancement of mesh sizing was practiced to have larger meshes in the center. The straight walls container was meshed by a homogenous system of  $1\text{mm}^3$  cubes. Although it had coarser meshes, having a homogenous shape, it was possible to cope with a better non-awkward geometry which needed a truly smaller computational time step.

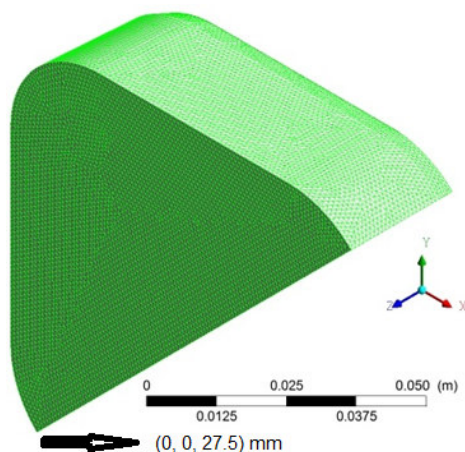


**Figure 2.** Straight wall container meshed geometry.

### Physical Properties

The properties of the carrot-orange soup were used according to the values reported by Rahman (1995) and Hayes (1987), based on mass fraction calculations. Density, specific heat, volume expansion coefficient and thermal conductivity were assumed constant. The viscosity was assumed Newtonian and as a function of temperature



in a form of second order polynomial Equation, [Equation (1)] (Steffe *et al.*, 1986). The temperature and viscosity values were reported by Ghani *et al.* (2001, 2002b) (Table 1).

$$\mu = a + bT + cT^2 \quad (1)$$

Where a, b and c are polynomial constants as indicated in table 1 and T is absolute temperature (K).

### Time-temperature Profile of the Retort

Time-Temperature profile of water cascading Barriquand steriflow (Roanne<sup>TM</sup>) retort, made in France, was measured by a thermocouple attached to Ellab data logger CTF9004 with PT100 cables to collect retort temperature in one minute time intervals. The data logger was connected to a PC. E-val software (version 2-1) was used to report and then export the data as a Microsoft excel file. The can outer surface (top, bottom and side walls) temperature is assumed equal to retort temperature throughout the whole sterilization period (Figure 8). The heating stage was simulated for 5,100 seconds. It took 10 steps to achieve the first 600 seconds of heating (come-up time), another 29 steps to reach 1,740 seconds (holding) and 46 steps for the rest of 5,100 seconds of sterilization period (cooling). As temperature is variable in warm up and cooling stages, time steps of 60 seconds were supposed and the retort temperature in each minute was applied to can outer surface in each time step but during holding stage, retort holding temperature was applied to can outer surface for all 29 steps of holding.

### SHZ and Lethality Estimation

**Table 1.** Physical properties of carrot-orange soup.

| Property  | Value                             |
|---|-----------------------------------|
| Density (kg m <sup>-3</sup> )                             | 1026                              |
| Specific heat (Jkg <sup>-1</sup> K <sup>-1</sup> )        | 3880                              |
| Thermal conductivity (W m <sup>-1</sup> K <sup>-1</sup> ) | 0.596                             |
| Volumetric expansion coefficient (K <sup>-1</sup> )       | 0.0002                            |
| Viscosity (Pa s)  | $\mu = 1.165T^2 - 8.145T + 16.77$ |

The coldest grid for WWC and SWC against other parts of geometry was found during the process. The temperature value of the coldest point at the end of each time step of processing period was used to calculate the lethality value based on the z value of 10°C, which refers to temperature required to change thermal death time by a factor of 10 for *Clostridium botulinum*, at each time step [Equation (2)]. The lethality values of coldest grid for both geometries were compared with each other by t student test.

$$Lethality = 10^{(T-121.1)/z} \quad (2)$$

Where, 121.1°C is the reference temperature and T is the predicted temperature in the coldest point of the can and z is 10°C.

### Heat Profile Analysis

The average temperature of the coldest zone on the symmetric plane was calculated at each time step and compared by the t student test.

### Governing Equations

The partial differential equations governing natural convection motion of fluid in a three-dimensional can are continuity, energy conservation and momentum equations in x, y and z coordinates as shown below and can be found in detail in (Versteeg and Malalasekera, 1995).

Continuity equation:

$$\frac{\partial u_x}{\partial x} + \frac{\partial u_y}{\partial y} + \frac{\partial u_z}{\partial z} = 0 \quad (3)$$

Energy conservation:

$$\frac{\partial T}{\partial t} + u_x \frac{\partial T}{\partial x} + u_y \frac{\partial T}{\partial y} + u_z \frac{\partial T}{\partial z} = \alpha \left( \frac{\partial^2 T}{\partial x^2} + \frac{\partial^2 T}{\partial y^2} + \frac{\partial^2 T}{\partial z^2} \right) \quad (4)$$

Momentum equation in three dimensions:  
 $x$ ,  $y$  and  $z$  components of momentum equation:

$$\left(\frac{\partial \rho V}{\partial t} + \nabla \cdot \rho V \otimes V\right) = \nabla \cdot (-p\delta + \mu(\nabla V + (\nabla V)^t)) + S_M \quad (5)$$

Buoyancy force caused by density variations due to temperature was assumed to be governed by Boussinesq approximation:

$$S_M = -\rho_{ref}\beta(T - T_{ref}) \quad (6)$$

Where  $\rho_{ref}$  is the reference density at temperature  $T_{ref}$  and  $\beta$  is the linear thermal expansion coefficient.

The Rayleigh is a dimensionless number which measures the strength of buoyancy driven flows. The product of the Grashof number and the Prandtl number gives the Rayleigh number that characterizes convection problems in heat transfer. Rayleigh number was lower than  $10^8$  and showed laminar flow during the process (Erdogdu and Tutar, 2011).

### Boundary Conditions and Initial Values

No-slip boundary condition was assumed for velocity components relative to boundaries (Kannan and Sandaka, 2008). Average come-up time was about 10 minutes and the temperature values were recorded in 60 second intervals which was used as time step intervals for the transient solution (Kumar and Bhattacharya, 1991). The condensing steam was assumed to provide constant boundary temperatures at the can outer surface (Ghani *et al.*, 1999; Ghani *et al.* 2001; Farid and Ghani, 2004). The boundary conditions used in the simulation were:  $T = T_w$ ,  $u = 0$ ,  $v = 0$ ,  $w = 0$  at the imposed sidewalls. The small bases of containers were assumed putting downward during the process. Initial temperature of food at the beginning of process was 328.15 K. Initial velocity components were:  $u = 0$ ,  $v = 0$ ,  $w = 0$ . The heating medium in the retort maintains a constant temperature condition at the can outer surface in the holding stage of sterilization while providing variable

temperature condition at the can outer surface in warm up and cooling stages of sterilization. These conditions were applied to can outer surface in each time step exactly. The thermal boundary conditions are applied to liquid boundaries rather than the outer boundaries of the can. This is correct since the can is composed of very thin layers of rotogravure print, stove lacquer white, aluminum foil, adhesive (aromatic polyurethane) and polypropylene film with a total thickness less than 0.15 mm and very small thermal resistance that was assumed negligible. Further the temperature at the liquid boundaries is assumed to reach boundary temperature from the initial conditions without any lag (Varma and Kannan, 2006).

### Solution Methodology

Ansys fluent (version 12, Ansys Inc., USA) was used to solve the Navier-Stokes and energy equations simultaneously to achieve a good convergence based on the value of residuals root mean square (RMS) lower than  $10^{-4}$  for continuity and momentum and  $10^{-8}$  for the energy equations. Applying good under-relaxation parameters will help to obtain a good convergence of the numerical solution. The under-relaxation factors were assumed smaller than 1. The PISO algorithm was used for pressure-velocity coupling. The simulation was carried out by a Sony VGN-BZ560 Vaio laptop with 2.4 GHz CPU speed and 2 GB RAM. The total simulation time performed about 22 hours (32,000 iterations) and 2 hours (2,800 iterations) for WWC and SWC, respectively.

## RESULTS AND DISCUSSION

### Mesh Optimization

To evaluate the correct decision about mesh size of the geometries, both of the designed packages had been meshed half and double size of the main mesh. In all cases, there was no significant differences

between the calculated temperatures in geometric center of the symmetric plate and 1 mm from each wall. As a result, the mentioned mesh sizes were seemed to be suitable.

### Fluid flow patterns

After 30 and 60 minutes of processing, the velocity ranged from  $2.18 \times 10^{-15}$  to  $2.87 \times 10^{-10} \text{ m s}^{-1}$  and from  $2.08 \times 10^{-15}$  to  $3.34 \times 10^{-10} \text{ m s}^{-1}$  for WWC, respectively. For SWC, this range was  $2.05 \times 10^{-15}$  to  $2.62 \times 10^{-10}$  and  $1.99 \times 10^{-15}$  to  $3.18 \times 10^{-10} \text{ m s}^{-1}$ . The velocity profiles were in a good agreement with studies by Ghani *et al.* (2002b) and it seemed to be logical that the convection pattern be the dominant phenomenon taking place in the container. A fluid circulation was observed around the geometric center of the container (Figure 3). Ghani *et al.* (2001) discussed the upward flow production due to the buoyancy force that is caused by a change in fluid density due to temperature variations. It was reported that, while processing, the hot fluid goes up and then travels toward the core. Velocity streamlines, as shown in Figure 4, show the circulation towards the walls in cooling time and holding process. After the fluid became heavier, the liquid in the core went down and then moved toward the walls, so a

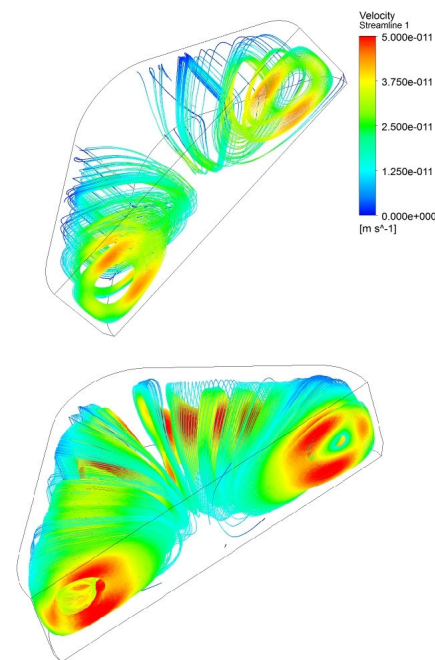


**Figure 4.** Velocity streamlines at 4,800 seconds (a) Wrinkled wall container, (b) Straight wall container.

circulation was taking place. At the end of holding-time, it seems that in the wrinkled wall containers the temperature distribution is almost homogenous and a very weak circulation is seen due to low buoyancy force. Twelve minutes after the holding time is finished ( $t = 60 \text{ min}$ ), the circulation direction became opposite in comparison to heating period. Because of higher

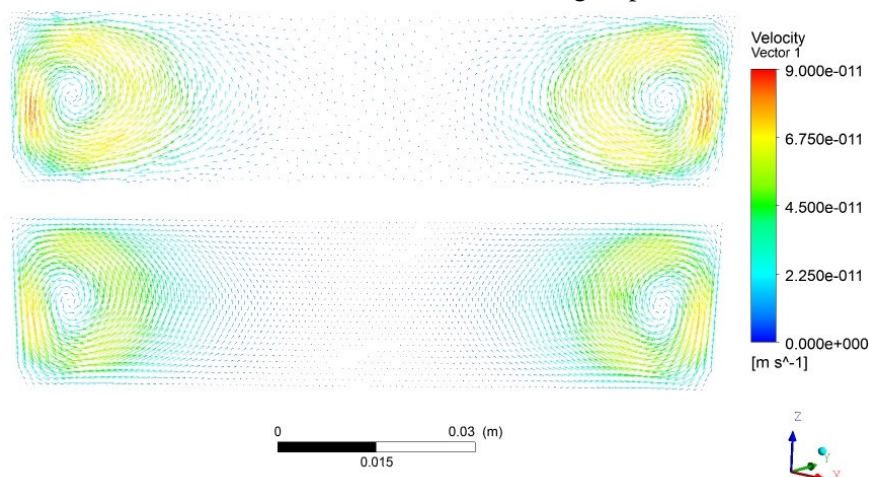


**Figure 3.** Velocity vectors of models in symmetric plane of wrinkled wall container (a) and straight wall container (b) at 420 seconds.

temperature average in the core, the fluid goes up and then moves towards the walls that have lower temperature. Being heavier, the liquid near the walls moves downwards the container and then goes towards the core.

### Temperature distribution

Temperature distribution of the middle plane of the containers ( $Z = 13.75$  mm) was shown at the last time step of come-up time (Figures 5-a and -b) and during the cooling process, after an hour of processing (Figures 5-c and -d).

The predicted area average temperature of the coldest point of the designed symmetric plane in WWC and the same location in SWC showed a high similarity (Figure 6). A paired comparison showed that temperature difference of the two points in symmetric plane was not significant ( $P < 0.01$ ). SHZ is the most important part of the metal containers specially when the fluid viscosity is high that would cause a high temperature difference in contrast to retort temperature (Zechman and Pflug, 1989). Varma and Kannan (2006) discussed that SHZ in convection cases does

not have a specific position (unlike in the conduction heat transfers that SHZ lies at the geometric center) and it is always moving due to the temperature distribution inside the container. The volume of liquid above the SHZ and the surface area below it would play important roles in the heat transfer (Varma and Kannan, 2006). In this study for both containers the volume of liquid above SHZ and the surface area below the SHZ were the same (as a function of container shape), thus as Table 2 shows, the SHZ was located in the same place in WWC and SWC. Ghani *et al.* (2002b) reported a migration of SHZ towards the bottom of the pouch into a region within 30-40% of the pouch height closest to its deepest end, but in this case since the geometry of the containers has a symmetric shape, the SHZ was located close to the geometric center of the containers during the process (Table 2). The processing must provide adequate heat treatment, in order to have enough lethality, imposed to the food container (Pflug, 1987).

### Microbial Thermal Destruction Calculations

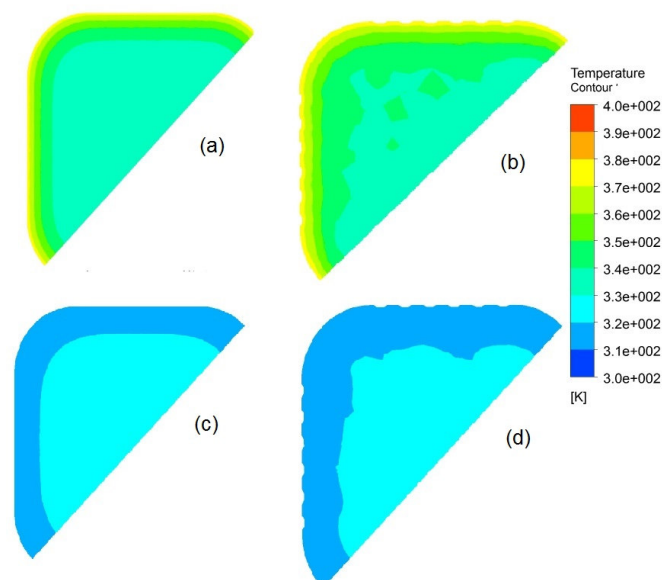


**Figure 5.** Temperature distribution in  $Z = 13.75$  mm (a, b): At 3,600 seconds for straight wall container and wrinkled wall container, respectively, and (c, d): At 48,000 seconds for straight wall container and wrinkled wall container, respectively.

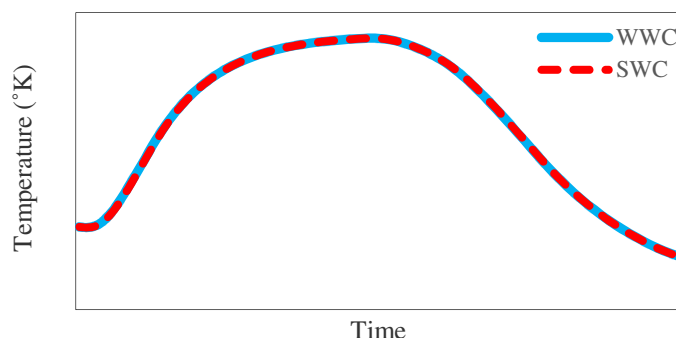


**Figure 6.** Predicted temperature of coldest point according to area average temperature in Wrinkled Wall Container (WWC) in contrast to the same position in Straight Wall Container (SWC).

**Table 2.** Cartesian location of the coldest point of SHZ based on the +x, +y, +z location of the container.

| Time (s) | (X, Y, Z) <sub>WWC</sub> <sup>a</sup> (mm) | (X, Y, Z) <sub>SWC</sub> <sup>b</sup> (mm) |
|----------|--|--|
| 720      | (46.978, 46.978, 13.848)                   | (43.887, 45.054, 13.792)                   |
| 1620     | (46.204, 46.204, 14.053)                   | (43.180, 44.348, 13.792)                   |
| 2520     | (44.318, 44.318, 13.750)                   | (43.180, 44.348, 13.792)                   |

<sup>a</sup> Wrinkled Wall Container, <sup>b</sup> Straight Wall Container.

The purpose of these calculations is to arrive at an appropriate process time under a given set of heating conditions to result in a given process lethality, or, alternately, to estimate the process lethality of a given process. The method used must accurately integrate the lethal effects of the transient temperature response of the food undergoing

the thermal processes with respect to the considered microorganism of both public health and spoilage concern (Khakbaz Heshmati *et al.*, 2014).

At the last time step of heating period (2,520 seconds), the lowest temperature point in WWC was chosen for heat treatment efficiency analysis in comparison

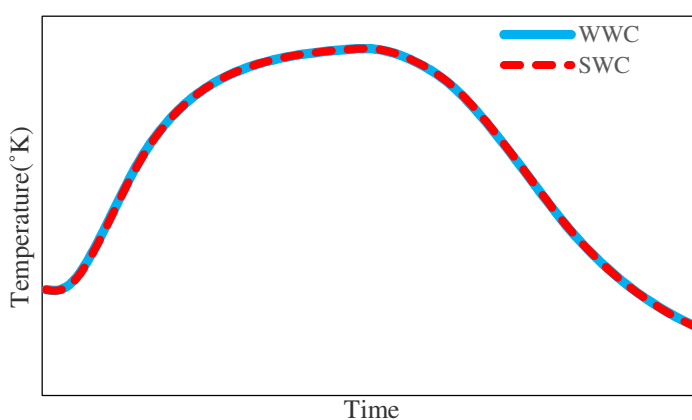


**Figure 7.** Predicted temperature of coldest point according to area average temperature in Wrinkled Wall Container (WWC) in contrast to the same location in Straight Wall Container (SWC).

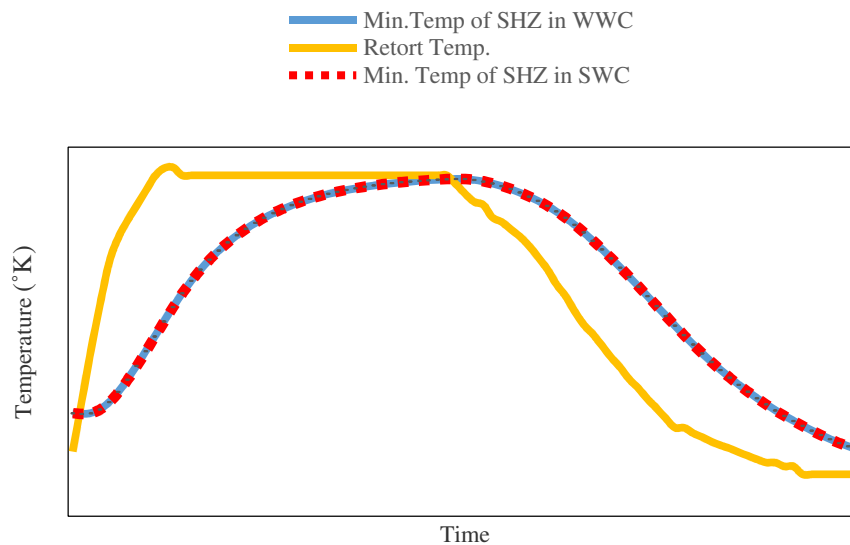


**Figure 8.** Time-temperature profile of retort and coldest point of SHZ in Wrinkled Wall Container (WWC) and Straight Wall Container (SWC).

with a point with the same location in SWC (Figure 7). This study was done on the lowest temperature point of SWC in contrast to the same position in WWC. *T*-test showed a high similarity about both cases ( $P < 0.05$ ). The total lethality values showed that WWC caused 0.4% more lethality than SWC.

## CONCLUSIONS

Two 3D geometrical models were designed, based on the B232 Alupak semi-rigid food containers, in order to study the effect of wrinkled wall design on temperature distribution of the containers. A mathematical model was developed by solving the governing equations for continuity, momentum and energy conservation using a finite volume method of solution. The average temperature of symmetric plane, SHZ movement and time-temperature distribution of the lowest temperature in SHZ were compared between the two cases. The results were in very good accordance to each other in spite of the large difference between the duration of computation of the cases. Hence, in order to

ease the geometry designing and to decrease the computation time, the geometry could be simplified.

## ACKNOWLEDGEMENTS

Chika International Food Industries are gratefully acknowledged for allowing the experimental work to be done.

## Nomenclature

|              |  |
|--------------|--|
| $C_p$        | Specific heat ( $\text{Jkg}^{-1} \text{K}^{-1}$ )                                      |
| $\text{div}$ | Divergence   |
| $g$          | Gravitational acceleration constant ( $\text{ms}^{-2}$ )                               |
| $k$          | Thermal conductivity of the liquid in the container ( $\text{Wm}^{-1} \text{K}^{-1}$ ) |
| $S_M$        | Source term for momentum   |
| $S_E$        | Source term for energy   |
| SHZ          | Slow Heating Zone  |
| SWC          | Straight Wall Container  |
| $t$          | Time of heating (s)  |
| $T$          | Temperature (K)  |
| $T_0$        | Initial temperature inside food container (K)  |
| $T_w$        | Wall temperature (K)   |



$V$  Velocity vector  
 $u$  Velocity in the  $X$ -direction ( $\text{m s}^{-1}$ )  
 $v$  Velocity in the  $Y$ -direction ( $\text{m s}^{-1}$ )  
 $w$  Velocity in the  $Z$ -direction ( $\text{m s}^{-1}$ )  
WWC Wrinkled Wall Container  
 $\beta$  thermal expansivity ( $\text{K}^{-1}$ )  
 $\delta$  Kronecker delta  
 $\mu$  Apparent viscosity ( $\text{Pa s}$ )  
 $\rho$  Density ( $\text{kg m}^{-3}$ )  
 $\rho_{\text{ref}}$  Density at the reference condition  
 $\tau$  Shear stress

## REFERENCES

1. Anandharamakrishnan, C., 2011. Applications of Computational Fluid Dynamics in Food Processing Operations, in: "Computational Fluid Dynamics: Theory, Analysis and Applications". Nova publishers, New York, pp. 297-316.
2. Bown, G. and Richardson, P. 2004. Modelling and Optimising Retort Temperature Control. Improving the thermal processing of foods 103-123.
3. Brody, A. L., 2002. Food Canning in the 21st century. *Food Technol.* **56**:75-78.
4. Chen, C. R., and Ramaswamy, H. S., 2007. Visual Basics Computer Simulation Package for Thermal Process Calculations. *Chem. Eng. Process.*, **46**: 603-613.
5. Datta, A. K. and Teixeira A. A 1988. Numerically Predicted Transient Temperature and Velocity Profiles during Natural Convection Heating of Canned Liquid Foods. *J. Food Sci.*, **53**:191-195.
6. Erdogdu, F. and Tutar, M., 2011. Velocity and Temperature Field Characteristics of Water and Air during Natural Convection Heating in Cans. *J. Food Sci.*, **76**:E119-E129.
7. Farid, M. M. and Ghani, A. G., 2004. A New Computational Technique for the Estimation of Sterilization Time in Canned Food. *Chemical Engineering and Processing: Process Intensification* **43**:523-531.
8. Ghani, A.G., Farid, M. M. and Chen, X. D., 2002a. Theoretical and Experimental Investigation of the Thermal Inactivation of *Bacillus stearothermophilus* in Food Pouches. *J. Food Eng.*, **51**:221-228.
9. Ghani, A. G., Farid, M. M. and Chen, X. D., 2002b. Theoretical and Experimental Investigation of the Thermal Destruction of Vitamin C in Food Pouches. *Comput. Electron. Agr.*, **34**:129-143.
10. Ghani, A. G., Farid, M. M. and Zarrouk, S. J., 2003. The effect of can rotation on sterilization of liquid food using computational fluid dynamics. *J. Food Eng.*, **57**:9-16.
11. Ghani, A. G. and Farid, M. M., 2006. Sterilization of Food in Retort Pouches. *springer*. 93-115
12. Ghani, A. G., Farid, M. M., Chen, X. D. and Richards, P., 1999. Numerical Simulation of Natural Convection Heating of Canned Food by Computational Fluid Dynamics. *J. Food Eng.*, **41**:55-64.
13. Ghani, A. G., Farid, M. M., Chen, X. D. and Richards, P., 2001. Thermal Sterilization of Canned Food in a 3-D Pouch Using Computational Fluid Dynamics. *J. Food Eng.*, **48**:147-156.
14. Hayes, G. D., 1987. Food Engineering Data Handbook. Wiley, New York. p. 55.
15. Kannan, A. and Sandaka, P., 2008. Heat Transfer Analysis of Canned Food Sterilization in a Still Retort. *J. Food Eng.*, **88**:213-228.
16. Khakbaz Heshmati, M., Shahedi, M., Hamdami, N., Hejazi, M. A., Motalebi, A. A. and Nasirpour, A., 2014. Mathematical Modeling of Heat Transfer and Sterilizing Value Evaluation during Caviar Pasteurization. *J. Agri. Sci. Technol.*, **16**: 827-839
17. Kiziltas, S., Erdogdu, F. and Palazoglu, T. K., 2010 Simulation of Heattransfer for Solid-liquid Food Mixtures in Cans and Model Validation under Pasteurization Conditions *J. Food Eng.*, **97**: 449-456.
18. Kumar, A., Bhattacharya, M. and Blaylock, J., 1990. Numerical Simulation of Natural Convection Heating of Canned Thick Viscous Liquid Food Products. *J. Food Sci.*, **55**:1403-1411.
19. Kumar, A. and Bhattacharya, M., 1991. Transient Temperature and Velocity Profiles in a Canned Non-Newtonian Liquid Food during Sterilization in a Still-cook Retort. *Int. J. Heat Mass Tran.*, **34**:1083-1096.
20. Naveh, D., Kopelman, I. J. and Pflug, I. J., 1983. The Finite Element Method in Thermal Processing of Foods. *J. Food Sci.*, **48**:1086-1093.

21. Nicolai, B. M., Verboven, P., Scheerlinck, N. and De Baerdemaeker, J., 1998. Numerical Analysis of the Propagation of Random Parameter Fluctuations in Time and Space during Thermal Food Processes. *J. Food Eng.*, **38**: 259-278.
22. Pflug, I. J., 1987. A Textbook for Introductory Course in Microbiology and Engineering of Sterilization, 6th edn. Minneapolis, Minnesota, Environmental Sterilization Laboratory.
23. Rahman, R., 1995. Food Properties Handbook. Boca Raton, CRC Press.
24. Ramesh, M. N., 2007. Canning and Sterilization of Foods. CRC Press. 585-625.
25. Steffe, J. F., Mohamed, I. O. and Ford, E. W., 1986. Physical and Chemical Properties of Foods. Transaction of American Society of Agricultural Engineers, St. Joseph, MI.
26. Teixeira, A. A., Dixon, J. R., Zahradnik, J. W. and Zinsmeister, G. E., 1969. Computer Optimization of Nutrient Retention in the Thermal Processing of Conduction-heated Foods. *Food Technol.*, **23**:134-140.
27. Varma, M. N. and Kannan, A., 2006. CFD Studies on Natural Convective Heating of Canned Food in Conical and Cylindrical Containers. *J. Food Eng.*, **77**:1024-1036.
28. Versteeg, H. K. and Malalasekera, W., 1995. An Introduction to Computational Fluid Dynamics the Finite Volume Method Longman Group Ltd. London, England.
29. Zechman, L. G. and Pflug, I. J., 1989. Location of the Slowest Heating Zone for Natural-Convection-Heating Fluids in Metal Containers. *J. Food Sci.*, **54**:205-209.

## ساده سازی هندسه بسته های نیمه انعطاف پذیر آلومینیومی دارای دیواره موج در شبیه سازی فرایند انتقال حرارت

ح. وطن خواه، ن. زمیندار، و م. شاهدی

### چکیده

ظروف آلومینیومی نیمه انعطاف پذیر به طور گسترده در صنعت مورد استفاده قرار می گیرند. این بسته بندی ها دارای دیواره های موج هستند که مقاومت فیزیکی ساختمان شان را افزایش می دهد. در این پژوهش، تاثیر وجود این دیواره ها بر انتقال حرارت و توزیع دمایی در شبیه سازی به روش دینامیک سیالات محاسباتی مورد بررسی قرار گرفته است. بدین منظور هندسه ظرف با دقت بالا طراحی و سپس با ظرف دارای دیواره ساده با ابعاد مشابه مقایسه شد. محتوای داخل ظرف، سوپ هویج-پرتقال در نظر گرفته شد. بردارهای سرعت نشان دهنده جریان حرارتی جابجایی به صورت چرخشی به سمت مرکز قوطی بود. تفاوت محل نقطه سرد هردو مدل در تمام طول فرآیند حرارتی کمتر از ۱٪ بود. میزان کشندگی اعمال شده در این نقطه برای میکروب کلستریدیوم بوتولینوم در هر دو مدل ۰/۴٪ اختلاف داشت. نتایج این شبیه سازی مشخص کرد اثر دیواره های موج بر انتقال حرارت معنی دار نیست.